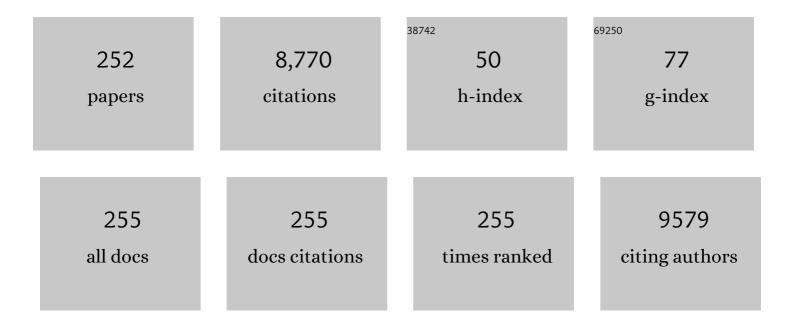
List of Publications by Year in descending order

Source: https://exaly.com/author-pdf/6395723/publications.pdf Version: 2024-02-01



#	Article	IF	CITATIONS
1	Material Characterization and Electrochemical Performance of Hydrous Manganese Oxide Electrodes for Use in Electrochemical Pseudocapacitors. Journal of the Electrochemical Society, 2003, 150, A1333.	2.9	254
2	Nano-architectured Co(OH)2 electrodes constructed using an easily-manipulated electrochemical protocol for high-performance energy storage applications. Journal of Materials Chemistry, 2010, 20, 3729.	6.7	228
3	Graphene nanosheets, carbon nanotubes, graphite, and activated carbon as anode materials for sodium-ion batteries. Journal of Materials Chemistry A, 2015, 3, 10320-10326.	10.3	216
4	A Honeycomb-like Co@N–C Composite for Ultrahigh Sulfur Loading Li–S Batteries. ACS Nano, 2017, 11, 11417-11424.	14.6	211
5	High entropy spinel oxide nanoparticles for superior lithiation–delithiation performance. Journal of Materials Chemistry A, 2020, 8, 18963-18973.	10.3	164
6	Dicyanamide anion based ionic liquids for electrodeposition of metals. Electrochemistry Communications, 2008, 10, 213-216.	4.7	151
7	Electrodeposition of aluminum on magnesium alloy in aluminum chloride (AlCl3)–1-ethyl-3-methylimidazolium chloride (EMIC) ionic liquid and its corrosion behavior. Electrochemistry Communications, 2007, 9, 1602-1606.	4.7	146
8	Electrochemical performance of Na/NaFePO4 sodium-ion batteries with ionic liquid electrolytes. Journal of Materials Chemistry A, 2014, 2, 5655.	10.3	142
9	Graphene grown on stainless steel as a high-performance and ecofriendly anti-corrosion coating for polymer electrolyte membrane fuel cell bipolar plates. Journal of Power Sources, 2015, 282, 248-256.	7.8	140
10	An entirely electrochemical preparation of a nano-structured cobalt oxide electrode with superior redox activity. Nanotechnology, 2009, 20, 175602.	2.6	137
11	Effect of heat treatment on material characteristics and pseudo-capacitive properties of manganese oxide prepared by anodic deposition. Journal of Power Sources, 2004, 135, 344-353.	7.8	136
12	Manganese oxide/carbon composite electrodes for electrochemical capacitors. Electrochemistry Communications, 2004, 6, 666-671.	4.7	135
13	In situ Mn K-edge X-ray absorption spectroscopic studies of anodically deposited manganese oxide with relevance to supercapacitor applications. Journal of Power Sources, 2007, 166, 590-594.	7.8	114
14	Physicochemical properties and electrochemical behavior of binary manganese–cobalt oxide electrodes for supercapacitor applications. Materials Chemistry and Physics, 2008, 108, 124-131.	4.0	104
15	Rechargeable Na/Na0.44MnO2 cells with ionic liquid electrolytes containing various sodium solutes. Journal of Power Sources, 2015, 274, 1016-1023.	7.8	102
16	High dispersion of 1-nm SnO2 particles between graphene nanosheets constructed using supercritical CO2 fluid for sodium-ion battery anodes. Nano Energy, 2016, 28, 124-134.	16.0	101
17	High-performance electrochemical pseudo-capacitor based on MnO2 nanowires/Ni foam as electrode with a novel Li-ion quasi-ionic liquid as electrolyte. Energy and Environmental Science, 2011, 4, 3942.	30.8	96
18	Formation of Nanoporous Nickel by Selective Anodic Etching of the Nobler Copper Component from Electrodeposited Nickelâ^'Copper Alloys. Journal of Physical Chemistry C, 2008, 112, 1371-1376.	3.1	95

#	Article	IF	CITATIONS
19	X-ray Photoelectron Spectroscopy and in Situ X-ray Absorption Spectroscopy Studies on Reversible Insertion/Desertion of Dicyanamide Anions into/from Manganese Oxide in Ionic Liquid. Chemistry of Materials, 2009, 21, 2688-2695.	6.7	95
20	Facile synthesis of silk-cocoon S-rich cobalt polysulfide as an efficient catalyst for the hydrogen evolution reaction. Energy and Environmental Science, 2018, 11, 2467-2475.	30.8	91
21	A facile approach to produce holey graphene and its application in supercapacitors. Carbon, 2015, 81, 347-356.	10.3	89
22	Annealed Mn–Fe binary oxides for supercapacitor applications. Journal of Power Sources, 2008, 185, 1550-1556.	7.8	86
23	Ionic Liquid Electrolytes with Various Sodium Solutes for Rechargeable Na/NaFePO ₄ Batteries Operated at Elevated Temperatures. ACS Applied Materials & Interfaces, 2014, 6, 17564-17570.	8.0	84
24	Titanium Carbide (MXene) as a Current Collector for Lithium-Ion Batteries. ACS Omega, 2018, 3, 12489-12494.	3.5	77
25	Electrochemical performance of MIL-53(Fe)@RGO as an Organic Anode Material for Li-ion Batteries. Electrochimica Acta, 2017, 246, 528-535.	5.2	76
26	Microwave growth and tunable photoluminescence of nitrogen-doped graphene and carbon nitride quantum dots. Journal of Materials Chemistry C, 2019, 7, 5468-5476.	5.5	75
27	MoS ₂ /graphene cathodes for reversibly storing Mg ²⁺ and Mg ²⁺ /Li ⁺ in rechargeable magnesium-anode batteries. Chemical Communications, 2016, 52, 1701-1704.	4.1	74
28	Moderately concentrated electrolyte improves solid–electrolyte interphase and sodium storage performance of hard carbon. Energy Storage Materials, 2019, 16, 146-154.	18.0	73
29	Tightly connected MnO2–graphene with tunable energy density and power density for supercapacitor applications. Journal of Materials Chemistry, 2012, 22, 7697.	6.7	72
30	Fluorescence of functionalized graphene quantum dots prepared from infrared-assisted pyrolysis of citric acid and urea. Journal of Luminescence, 2020, 217, 116774.	3.1	72
31	Electrodeposition behavior of nickel in the water- and air-stable 1-ethyl-3-methylimidazolium-dicyanamide room-temperature ionic liquid. Electrochimica Acta, 2008, 53, 5812-5818.	5.2	70
32	lonic-liquid-enhanced glucose sensing ability of non-enzymatic Au/graphene electrodes fabricated using supercritical CO2 fluid. Biosensors and Bioelectronics, 2013, 46, 30-36.	10.1	68
33	Ionic Liquid Electrolytes with Various Constituent Ions for Graphene-based Supercapacitors. Electrochimica Acta, 2015, 161, 371-377.	5.2	65
34	Manganese films electrodeposited at different potentials and temperatures in ionic liquid and their application as electrode materials for supercapacitors. Electrochimica Acta, 2008, 53, 4447-4453.	5.2	63
35	Electrochemistry of Zn(II)/Zn on Mg alloy from the N-butyl-N-methylpyrrolidinium dicyanamide ionic liquid. Electrochimica Acta, 2011, 56, 6071-6077.	5.2	61
36	ZIF-8-Based Quasi-Solid-State Electrolyte for Lithium Batteries. ACS Applied Materials & Interfaces, 2019, 11, 46671-46677.	8.0	61

#	Article	IF	CITATIONS
37	Physicochemical factors that affect the pseudocapacitance and cyclic stability of Mn oxide electrodes. Electrochimica Acta, 2009, 54, 3278-3284.	5.2	59
38	Pseudocapacitive Mechanism of Manganese Oxide in 1-Ethyl-3-methylimidazolium Thiocyanate Ionic Liquid Electrolyte Studied Using X-ray Photoelectron Spectroscopy. Langmuir, 2009, 25, 11955-11960.	3.5	59
39	Supercritical CO ₂ â€Assisted SiO <i>_x</i> /Carbon Multiâ€Layer Coating on Si Anode for Lithiumâ€Ion Batteries. Advanced Functional Materials, 2021, 31, 2104135.	14.9	59
40	Thermal conductivity from hierarchical heat sinks using carbon nanotubes and graphene nanosheets. Nanoscale, 2015, 7, 18663-18670.	5.6	58
41	Highly enhanced electrochemical performance of ultrafine CuO nanoparticles confined in ordered mesoporous carbons as anode materials for sodium-ion batteries. Journal of Materials Chemistry A, 2016, 4, 14222-14233.	10.3	58
42	Tailoring fluorescence emissions, quantum yields, and white light emitting from nitrogen-doped graphene and carbon nitride quantum dots. Nanoscale, 2019, 11, 16553-16561.	5.6	57
43	Ideal pseudocapacitive performance of the Mn oxide anodized from the nanostructured and amorphous Mn thin film electrodeposited in BMP–NTf2 ionic liquid. Journal of Power Sources, 2008, 179, 435-440.	7.8	56
44	Decorating carbon nanotubes with Ni particles using an electroless deposition technique for hydrogen storage applications. International Journal of Hydrogen Energy, 2010, 35, 7555-7562.	7.1	56
45	Corrosion characteristics of nickel, copper, and stainless steel in a Lewis neutral chloroaluminate ionic liquid. Corrosion Science, 2011, 53, 4318-4323.	6.6	53
46	Atomic-scale investigation of Lithiation/Delithiation mechanism in High-entropy spinel oxide with superior electrochemical performance. Chemical Engineering Journal, 2021, 420, 129838.	12.7	53
47	Microstructure and Pseudocapacitive Performance of Anodically Deposited Manganese Oxide with Various Heat-Treatments. Journal of the Electrochemical Society, 2005, 152, A2063.	2.9	52
48	A novel electrochemical process to prepare a high-porosity manganese oxide electrode with promising pseudocapacitive performance. Journal of Power Sources, 2008, 177, 676-680.	7.8	52
49	Uranium In Situ Electrolytic Deposition with a Reusable Functional Grapheneâ€Foam Electrode. Advanced Materials, 2021, 33, e2102633.	21.0	52
50	Improved supercapacitor performance of MnO2–graphene composites constructed using a supercritical fluid and wrapped with an ionic liquid. Journal of Materials Chemistry A, 2013, 1, 3395.	10.3	51
51	Correlations between electrochemical Na ⁺ storage properties and physiochemical characteristics of holey graphene nanosheets. Journal of Materials Chemistry A, 2015, 3, 17282-17289.	10.3	51
52	Electrochemically grown nanocrystalline V2O5 as high-performance cathode for sodium-ion batteries. Journal of Power Sources, 2015, 285, 418-424.	7.8	51
53	Suitability of ionic liquid electrolytes for room-temperature sodium-ion battery applications. Chemical Communications, 2016, 52, 10890-10893.	4.1	51
54	Effects of Iron Addition on Material Characteristics and Pseudo-Capacitive Behavior of Mn-Oxide Electrodes. Journal of the Electrochemical Society, 2007, 154, A875.	2.9	50

#	Article	IF	CITATIONS
55	Corrosion behaviors of materials in aluminum chloride–1-ethyl-3-methylimidazolium chloride ionic liquid. Electrochemistry Communications, 2010, 12, 1091-1094.	4.7	50
56	Co-free high entropy spinel oxide anode with controlled morphology and crystallinity for outstanding charge/discharge performance in Lithium-ion batteries. Chemical Engineering Journal, 2022, 430, 132658.	12.7	49
57	Co-deposition of Al–Zn on AZ91D magnesium alloy in AlCl3–1-ethyl-3-methylimidazolium chloride ionic liquid. Electrochimica Acta, 2010, 55, 2158-2162.	5.2	48
58	Carbonaceous Anodes Derived from Sugarcane Bagasse for Sodiumâ€lon Batteries. ChemSusChem, 2019, 12, 2302-2309.	6.8	48
59	Effects of Elemental Modulation on Phase Purity and Electrochemical Properties of Coâ€free Highâ€Entropy Spinel Oxide Anodes for Lithiumâ€ion Batteries. Advanced Functional Materials, 2022, 32, .	14.9	48
60	Improved Corrosion Resistance of Magnesium Alloy with a Surface Aluminum Coating Electrodeposited in Ionic Liquid. Journal of the Electrochemical Society, 2008, 155, C112.	2.9	44
61	Electrodeposition of Palladium–Copper Films from 1-Ethyl-3-methylimidazolium Chloride–Tetrafluoroborate Ionic Liquid on Indium Tin Oxide Electrodes. Journal of the Electrochemical Society, 2009, 156, D193.	2.9	44
62	Electroless deposition of Ni nanoparticles on carbon nanotubes with the aid of supercritical CO2 fluid and a synergistic hydrogen storage property of the composite. International Journal of Hydrogen Energy, 2010, 35, 5490-5497.	7.1	44
63	Uniform dispersion of Pd nanoparticles on carbon nanostructures using a supercritical fluid deposition technique and their catalytic performance towards hydrogen spillover. Journal of Materials Chemistry, 2011, 21, 19063.	6.7	44
64	Pseudocapacitive behavior of Mn oxide in aprotic 1-ethyl-3-methylimidazolium–dicyanamide ionic liquid. Journal of Materials Chemistry, 2009, 19, 3732.	6.7	43
65	Corrosion properties of metals in dicyanamide-based ionic liquids. Corrosion Science, 2014, 78, 81-88.	6.6	43
66	Holey Graphene Nanosheets with Surface Functional Groups as Highâ€Performance Supercapacitors in Ionicâ€Liquid Electrolyte. ChemSusChem, 2015, 8, 1779-1786.	6.8	43
67	Electrolyte Optimization for Enhancing Electrochemical Performance of Antimony Sulfide/Graphene Anodes for Sodium-Ion Batteries–Carbonate-Based and Ionic Liquid Electrolytes. ACS Sustainable Chemistry and Engineering, 2017, 5, 8269-8276.	6.7	43
68	Facile synthesis of core–shell structured Si@graphene balls as a high-performance anode for lithium-ion batteries. Nanoscale, 2020, 12, 9616-9627.	5.6	43
69	Fabrication of anode-supported thin BCZY electrolyte protonic fuel cells using NiO sintering aid. International Journal of Hydrogen Energy, 2019, 44, 23784-23792.	7.1	42
70	Unique Pd/graphene nanocomposites constructed using supercritical fluid for superior electrochemical sensing performance. Journal of Materials Chemistry, 2012, 22, 21466.	6.7	41
71	Infrared-assisted Synthesis of Lithium Nickel Cobalt Alumina Oxide Powders as Electrode Material for Lithium-ion Batteries. Electrochimica Acta, 2016, 206, 207-216.	5.2	41
72	Functional Group-Dependent Supercapacitive and Aging Properties of Activated Carbon Electrodes in Organic Electrolyte. ACS Sustainable Chemistry and Engineering, 2018, 6, 1208-1214.	6.7	41

#	Article	IF	CITATIONS
73	An oxygen-blocking oriented multifunctional solid–electrolyte interphase as a protective layer for a lithium metal anode in lithium–oxygen batteries. Energy and Environmental Science, 2021, 14, 1439-1448.	30.8	41
74	Pseudocapacitance of MnO2 originates from reversible insertion/desertion of thiocyanate anions studied using in situ X-ray absorption spectroscopy in ionic liquid electrolyte. Journal of Power Sources, 2010, 195, 919-922.	7.8	40
75	Improved pseudocapacitive performance and cycle life of cobalt hydroxide on an electrochemically derived nano-porous Ni framework. Journal of Power Sources, 2011, 196, 7828-7834.	7.8	40
76	Doped butylmethylpyrrolidinium–dicyanamide ionic liquid as an electrolyte for MnO2 supercapacitors. Journal of Materials Chemistry, 2012, 22, 6274.	6.7	40
77	A functionalized membrane for lithium–oxygen batteries to suppress the shuttle effect of redox mediators. Journal of Materials Chemistry A, 2019, 7, 14260-14270.	10.3	40
78	Effects of Temperature and Concentration on the Structure and Specific Capacitance of Manganese Oxide Deposited in Manganese Acetate Solution. Journal of Applied Electrochemistry, 2004, 34, 953-961.	2.9	39
79	High energy density of all-screen-printable solid-state microsupercapacitors integrated by graphene/CNTs as hierarchical electrodes. Journal of Materials Chemistry A, 2019, 7, 12779-12789.	10.3	38
80	A Novel Moistureâ€Insensitive and Lowâ€Corrosivity Ionic Liquid Electrolyte for Rechargeable Aluminum Batteries. Advanced Functional Materials, 2020, 30, 1909565.	14.9	38
81	Charge-storage performance of Li/LiFePO4 cells with additive-incorporated ionic liquid electrolytes at various temperatures. Journal of Power Sources, 2014, 260, 268-275.	7.8	37
82	The proton conduction and hydrogen permeation characteristic of Sr(Ce0.6Zr0.4)0.85Y0.15O3â^'Î′ ceramic separation membrane. Journal of the European Ceramic Society, 2015, 35, 163-170.	5.7	37
83	Comparative Study on the Morphology-Dependent Performance of Various CuO Nanostructures as Anode Materials for Sodium-Ion Batteries. ACS Sustainable Chemistry and Engineering, 2018, 6, 10876-10885.	6.7	37
84	Effects of the Co content in the material characteristics and supercapacitive performance of binary Mn–Co oxide electrodes. Journal of Alloys and Compounds, 2008, 461, 667-674.	5.5	35
85	High-selectivity electrochemical non-enzymatic sensors based on graphene/Pd nanocomposites functionalized with designated ionic liquids. Biosensors and Bioelectronics, 2017, 89, 483-488.	10.1	34
86	A Waterâ€Soluble NaCMC/NaPAA Binder for Exceptional Improvement of Sodiumâ€Ion Batteries with an SnO ₂ â€Ordered Mesoporous Carbon Anode. ChemSusChem, 2018, 11, 3923-3931.	6.8	34
87	High reversible Li plating and stripping by in-situ construction a multifunctional lithium-pinned array. Energy Storage Materials, 2020, 28, 188-195.	18.0	34
88	Diameter-sensitive biocompatibility of anodic TiO2 nanotubes treated with supercritical CO2 fluid. Nanoscale Research Letters, 2013, 8, 150.	5.7	33
89	Three-dimensional interpenetrating mesoporous carbon confining SnO ₂ particles for superior sodiation/desodiation properties. Nanoscale, 2017, 9, 8674-8683.	5.6	33
90	Electrochemical Characteristics of a Polymer/Garnet Trilayer Composite Electrolyte for Solid-State Lithium-Metal Batteries. ACS Applied Materials & Interfaces, 2021, 13, 2507-2520.	8.0	33

#	Article	IF	CITATIONS
91	Gravimetric/volumetric capacitances, leakage current, and gas evolution of activated carbon supercapacitors. Electrochimica Acta, 2016, 222, 1153-1159.	5.2	32
92	Hybrid electrolyte enables safe and practical 5 V LiNi _{0.5} Mn _{1.5} O ₄ batteries. Journal of Materials Chemistry A, 2019, 7, 16516-16525.	10.3	32
93	Highly concentrated carbonate electrolyte for Li-ion batteries with lithium metal and graphite anodes. Journal of Power Sources, 2020, 450, 227657.	7.8	32
94	Manipulation of Nitrogen-Heteroatom Configuration for Enhanced Charge-Storage Performance and Reliability of Nanoporous Carbon Electrodes. ACS Applied Materials & Interfaces, 2020, 12, 32797-32805.	8.0	32
95	BaZr0.2Ce0.8â^'xYxO3â^'Î′ solid oxide fuel cell electrolyte synthesized by sol–gel combined with composition-exchange method. International Journal of Hydrogen Energy, 2014, 39, 14434-14440.	7.1	30
96	Strontium doping effect on phase homogeneity and conductivity of Ba1â^'xSrxCe0.6Zr0.2Y0.2O3â^'δ proton-conducting oxides. International Journal of Hydrogen Energy, 2013, 38, 11097-11103.	7.1	29
97	Manipulation of Heteroatom Substitution on Nitrogen and Phosphorus Co-Doped Graphene as a High Active Catalyst for Hydrogen Evolution Reaction. Journal of Physical Chemistry C, 2019, 123, 22202-22211.	3.1	29
98	Ionic liquid electrolytes for high-voltage rechargeable Li/LiNi0.5Mn1.5O4 cells. Journal of Materials Chemistry A, 2014, 2, 3613.	10.3	28
99	In situ atomic scale investigation of Li7La3Zr2O12-based Li+-conducting solid electrolyte during calcination growth. Nano Energy, 2020, 71, 104625.	16.0	28
100	An interfacial wetting water based hydrogel electrolyte for high-voltage flexible quasi solid-state supercapacitors. Energy Storage Materials, 2021, 38, 489-498.	18.0	28
101	Charge–Discharge Mechanism of Highâ€Entropy Coâ€Free Spinel Oxide Toward Li ⁺ Storage Examined Using Operando Quickâ€Scanning Xâ€Ray Absorption Spectroscopy. Advanced Science, 2022, 9, .	11.2	28
102	Effects of Co, Mn contents on the electrochemical characteristics of the LaNi3.8(Co + Mn)0.96Al0.24 electrodes in potassium hydroxide electrolyte. Journal of Power Sources, 2002, 103, 280-285.	7.8	27
103	Electrodeposition of Palladium–Tin Alloys from 1-Ethyl-3-methylimidazolium Chloride–Tetrafluoroborate Ionic Liquid for Ethanol Electro-Oxidation. Journal of the Electrochemical Society, 2010, 157, D443.	2.9	27
104	Nanostructured Na-doped vanadium oxide synthesized using an anodic deposition technique for supercapacitor applications. Journal of Alloys and Compounds, 2012, 536, S428-S431.	5.5	27
105	Electrochemical performance of rechargeable Li/LiFePO4 cells with ionic liquid electrolyte: Effects of Li salt at 25ŰC and 50ŰC. Journal of Power Sources, 2013, 240, 676-682.	7.8	27
106	Improvement of the Electrochemical Characteristics of Lithium and Manganese Rich Layered Cathode Materials: Effect of Surface Coating. Journal of the Electrochemical Society, 2015, 162, A1957-A1965.	2.9	27
107	A polyoxometalate-based polymer electrolyte with an improved electrode interface and ion conductivity for high-safety all-solid-state batteries. Journal of Materials Chemistry A, 2019, 7, 15924-15932.	10.3	27
108	The advent of manganese-substituted sodium vanadium phosphate-based cathodes for sodium-ion batteries and their current progress: a focused review. Journal of Materials Chemistry A, 2022, 10, 1022-1046.	10.3	26

#	Article	IF	CITATIONS
109	Enhancing hydrogen storage on carbon nanotubes via hybrid chemical etching and Pt decoration employing supercritical carbon dioxide fluid. International Journal of Hydrogen Energy, 2012, 37, 6714-6720.	7.1	25
110	The effects of ionic liquid on the electrochemical sensing performance of graphene- and carbon nanotube-based electrodes. Analyst, The, 2013, 138, 576-582.	3.5	25
111	Optimizing the Mg Doping Concentration of Na ₃ V _{2–<i>x</i>} Mg _{<i>x</i>} (PO ₄) ₂ F _{3<!--<br-->for Enhanced Sodiation/Desodiation Properties. ACS Sustainable Chemistry and Engineering, 2021, 9, 6962-6971.}	sub>/C 6.7	25
112	Heat-treatment induced material property variations of Al-coated Mg alloy prepared in aluminum chloride/1-ethyl-3-methylimidazolium chloride ionic liquid. Surface and Coatings Technology, 2010, 205, 200-204.	4.8	24
113	Microstructure and Electrochemical Characteristics of Aluminum Anodized Film Formed in Ammonium Adipate Solution. Journal of the Electrochemical Society, 2003, 150, B266.	2.9	23
114	In situ X-ray absorption spectroscopic studies of anodically deposited binary Mn–Fe mixed oxides with relevance to pseudocapacitance. Journal of Power Sources, 2008, 178, 476-482.	7.8	23
115	Fabrication of Porous Tin by Template-Free Electrodeposition of Tin Nanowires from an Ionic Liquid. Electrochemical and Solid-State Letters, 2008, 11, D85.	2.2	23
116	Evaluation of Ionic Liquid Electrolytes for Use in Manganese Oxide Supercapacitors. Electrochemical and Solid-State Letters, 2009, 12, A19.	2.2	23
117	Buckyball-, carbon nanotube-, graphite-, and graphene-enhanced dehydrogenation of lithium aluminum hydride. Chemical Communications, 2013, 49, 8845.	4.1	23
118	Copolymers Based on 1,3-Bis(carbazol-9-yl)benzene and Three 3,4-Ethylenedioxythiophene Derivatives as Potential Anodically Coloring Copolymers in High-Contrast Electrochromic Devices. Polymers, 2016, 8, 368.	4.5	23
119	Scalable Patterning of MoS ₂ Nanoribbons by Micromolding in Capillaries. ACS Applied Materials & Interfaces, 2016, 8, 20993-21001.	8.0	23
120	The hierarchical porosity of a three-dimensional graphene electrode for binder-free and high performance supercapacitors. RSC Advances, 2016, 6, 8384-8394.	3.6	23
121	Synthesis of bimetallic sulfide FeCoS4@carbon nanotube graphene hybrid as a high-performance anode material for sodium-ion batteries. Chemical Engineering Journal, 2021, 423, 130070.	12.7	23
122	Tin phosphide-carbon composite as a high-performance anode active material for sodium-ion batteries with high energy density. Journal of Energy Chemistry, 2022, 64, 463-474.	12.9	23
123	Effect of Heat-Treatment on Characteristics of Anodized Aluminum Oxide Formed in Ammonium Adipate Solution. Journal of the Electrochemical Society, 2004, 151, B188.	2.9	22
124	Diffusion coefficients, spin-lattice relaxation times, and chemical shift variations of NMR spectra in LiTFSI-doped ether- and allyl-functionalized dicationic ionic liquids. Journal of the Taiwan Institute of Chemical Engineers, 2016, 60, 138-150.	5.3	22
125	Hydrogenated Anatase and Rutile TiO ₂ for Sodium-Ion Battery Anodes. ACS Applied Energy Materials, 2021, 4, 5738-5746.	5.1	22
126	Microplasma-assisted bottom-up synthesis of graphene nanosheets with superior sodium-ion storage performance. Journal of Materials Chemistry A, 2016, 4, 7624-7631.	10.3	21

#	Article	lF	CITATIONS
127	Electrochemical Na ⁺ storage properties of SnO ₂ /graphene anodes in carbonate-based and ionic liquid electrolytes. Journal of Materials Chemistry A, 2017, 5, 13776-13784.	10.3	21
128	Ecoâ€Efficient Synthesis of Highly Porous CoCO ₃ Anodes from Supercritical CO ₂ for Li ⁺ and Na ⁺ Storage. ChemSusChem, 2017, 10, 2464-2472.	6.8	21
129	Controlled multimodal hierarchically porous electrode self-assembly of electrochemically exfoliated graphene for fully solid-state flexible supercapacitor. Physical Chemistry Chemical Physics, 2017, 19, 30381-30392.	2.8	21
130	Facile fabrication of titania-ordered cubic mesoporous carbon composite: Effect of Ni doping on photocatalytic hydrogen generation. International Journal of Hydrogen Energy, 2019, 44, 19255-19266.	7.1	21
131	Composition manipulation of bis(fluorosulfonyl)imide-based ionic liquid electrolyte for high-voltage graphite//LiNi0.5Mn1.5O4 lithium-ion batteries. Chemical Engineering Journal, 2021, 415, 128904.	12.7	21
132	Preparation of Manganese Thin Film in Room-Temperature Butylmethylpyrrolidinium Bis(trifluoromethylsulfony)imide Ionic Liquid and Its Application for Supercapacitors. Electrochemical and Solid-State Letters, 2007, 10, A9.	2.2	20
133	Metal/graphene nanocomposites synthesized with the aid of supercritical fluid for promoting hydrogen release from complex hydrides. Nanoscale, 2014, 6, 12565-12572.	5.6	20
134	Three-dimensional carbon framework anode improves sodiation–desodiation properties in ionic liquid electrolyte. Nano Energy, 2018, 49, 515-522.	16.0	20
135	Supercapacitive Properties of Micropore―and Mesoporeâ€Rich Activated Carbon in Ionicâ€Liquid Electrolytes with Various Constituent Ions. ChemSusChem, 2019, 12, 449-456.	6.8	20
136	A comprehensive review on recent advances of polyanionic cathode materials in Naâ€ion batteries for cost effective energy storage applications. Wiley Interdisciplinary Reviews: Energy and Environment, 2021, 10, e400.	4.1	20
137	Room-Temperature Hydrogen Adsorption via Spillover in Pt Nanoparticle-Decorated UiO-66 Nanoparticles: Implications for Hydrogen Storage. ACS Applied Nano Materials, 2021, 4, 11269-11280.	5.0	20
138	Manganese oxide thin films prepared by potentiodynamic electrodeposition and their supercapacitor performance. Journal of Solid State Electrochemistry, 2010, 14, 1697-1703.	2.5	19
139	Structure and hydrogen storage properties of Mg2Cu1â^xNix (x=0–1) alloys. International Journal of Hydrogen Energy, 2010, 35, 13247-13254.	7.1	19
140	Pseudocapacitive behavior of manganese oxide in lithium-ion-doped butylmethylpyrrolidinium–dicyanamide ionic liquid investigated using in situ X-ray absorption spectroscopy. Journal of Power Sources, 2014, 246, 269-276.	7.8	19
141	Improved lithium storage capacity and high rate capability of nitrogen-doped graphite-like electrode materials prepared from thermal pyrolysis of graphene quantum dots. Electrochimica Acta, 2020, 354, 136642.	5.2	19
142	Fluorinated graphene as a dual-functional anode to achieve dendrite-free and high-performance lithium metal batteries. Carbon, 2022, 197, 141-151.	10.3	19
143	Effect of electrolyte composition on hydration resistance of anodized aluminum oxide. Journal of Power Sources, 2004, 138, 301-308.	7.8	18
144	Decorating carbon nanotubes with nanoparticles using a facile redox displacement reaction and an evaluation of synergistic hydrogen storage performance. Nanotechnology, 2009, 20, 495603.	2.6	18

#	Article	IF	CITATIONS
145	Improved hydrogen storage performance of defected carbon nanotubes with Pd spillover catalysts dispersed using supercritical CO2 fluid. International Journal of Hydrogen Energy, 2012, 37, 3305-3312.	7.1	18
146	Superior coulombic efficiency of lithium anodes for rechargeable batteries utilizing high-concentration ether electrolytes. Electrochimica Acta, 2019, 319, 625-633.	5.2	18
147	Composition Modulation of Ionic Liquid Hybrid Electrolyte for 5 V Lithium-Ion Batteries. ACS Applied Materials & Interfaces, 2019, 11, 42049-42056.	8.0	18
148	Ga-doped lithium lanthanum zirconium oxide electrolyte for solid-state Li batteries. Electrochimica Acta, 2020, 353, 136536.	5.2	18
149	Effects of surface functional groups of coal-tar-pitch-derived nanoporous carbon anodes on microbial fuel cell performance. Renewable Energy, 2021, 171, 87-94.	8.9	18
150	Effects of heat treatment on materials characteristics and hydrogen storage capability of multi-wall carbon nanotubes. Diamond and Related Materials, 2009, 18, 553-556.	3.9	17
151	Synthesis and characterization of Ba0.6Sr0.4Ce0.8â^xZrxY0.2O3â^î^r proton-conducting oxides for use as fuel cell electrolyte. Journal of Alloys and Compounds, 2014, 586, S506-S510.	5.5	17
152	Nanostructured tin electrodeposited in ionic liquid for use as an anode for Li-ion batteries. Journal of Materials Chemistry A, 2014, 2, 16547-16553.	10.3	17
153	Nanocrystalline Pd/carbon nanotube composites synthesized using supercritical fluid for superior glucose sensing performance. Journal of Alloys and Compounds, 2014, 615, S496-S500.	5.5	17
154	Nanostructured poly(aniline-co-metanilic acid) as platinum catalyst support for electro-oxidation of methanol. International Journal of Hydrogen Energy, 2015, 40, 2631-2640.	7.1	17
155	Selective micro-etching of duplex stainless steel for preparing manganese oxide supercapacitor electrode. Journal of Power Sources, 2009, 187, 261-267.	7.8	16
156	Electrodeposition of Ni-Cu Alloys in an Air and Water Stable Room Temperature Ionic Liquid. Electrochemistry, 2009, 77, 582-584.	1.4	16
157	Electrochemical performance of 0.5Li2MnO3–0.5Li(Mn0.375Ni0.375Co0.25)O2 composite cathode inÂpyrrolidinium-based ionic liquid electrolytes. Journal of Power Sources, 2015, 294, 22-30.	7.8	16
158	Poly(tris(4-carbazoyl-9-ylphenyl)amine)/Three Poly(3,4-ethylenedioxythiophene) Derivatives in Complementary High-Contrast Electrochromic Devices. Polymers, 2017, 9, 543.	4.5	16
159	Electrochromic Devices Based on Poly(2,6-di(9H-carbazol-9-yl)pyridine)-Type Polymer Films and PEDOT-PSS. Polymers, 2018, 10, 604.	4.5	16
160	Microstructures and electrical properties of zirconium doped barium cerate perovskite proton conductors. International Journal of Hydrogen Energy, 2019, 44, 21174-21180.	7.1	16
161	A metal dusting process for preparing nano-sized carbon materials and the effects of acid post-treatment on their hydrogen storage performance. International Journal of Hydrogen Energy, 2008, 33, 6734-6742.	7.1	15
162	Structure-mediated electrochemical performance of SnS 2 anode for Li-ion batteries. Journal of the Taiwan Institute of Chemical Engineers, 2016, 66, 292-300.	5.3	15

#	Article	IF	CITATIONS
163	Nanocatalyst-Assisted Fine Tailoring of Pore Structure in Holey-Graphene for Enhanced Performance in Energy Storage. ACS Applied Materials & Interfaces, 2019, 11, 36560-36570.	8.0	15
164	Ordered nano-structured mesoporous CMK-8 and other carbonaceous positive electrodes for rechargeable aluminum batteries. Chemical Engineering Journal, 2021, 417, 129131.	12.7	15
165	High-Li+-fraction ether-side-chain pyrrolidinium–asymmetric imide ionic liquid electrolyte for high-energy-density Si//Ni-rich layered oxide Li-ion batteries. Chemical Engineering Journal, 2022, 430, 132693.	12.7	15
166	Effect of Ni content on the electrochemical characteristics of the LaNi5-based hydrogen storage alloys. Materials Chemistry and Physics, 2004, 83, 361-366.	4.0	14
167	Synthesis and electrochemical properties of xLiFePO4·(1Â−Âx)LiVPO4F composites prepared by aqueous precipitation and carbothermal reduction. Journal of Power Sources, 2013, 244, 63-71.	7.8	14
168	Proton-conducting Ba1â^'xKxCe0.6Zr0.2Y0.2O3â~'δ oxides synthesized by sol–gel combined with composition-exchange method. Ceramics International, 2014, 40, 1865-1872.	4.8	14
169	Potassium doping optimization in proton-conducting Ba1-xKxCe0.6Zr0.2Y0.2O3-δ oxides for fuel cell applications. Journal of Alloys and Compounds, 2017, 696, 251-256.	5.5	14
170	Atomic layer oxidation on graphene sheets for tuning their oxidation levels, electrical conductivities, and band gaps. Nanoscale, 2018, 10, 15521-15528.	5.6	14
171	Tuning of Na+ Concentration in an Ionic Liquid Electrolyte to Optimize Solid–Electrolyte Interphase at Microplasma-Synthesized Graphene Anode for Na-Ion Batteries. ACS Sustainable Chemistry and Engineering, 2019, 7, 16682-16689.	6.7	14
172	Control of Graphene Heteroatoms in a Microball Si@Graphene Composite Anode for High-Energy-Density Lithium-Ion Full Cells. ACS Sustainable Chemistry and Engineering, 2020, 8, 18936-18946.	6.7	14
173	A Lithium-Ion Rechargeable Full Cell Using the Flower-like Na ₃ V ₂ (PO ₄) ₃ @C Cathode and Li ₄ Ti ₅ O ₁₂ Anode. ACS Sustainable Chemistry and Engineering, 2020, 8, 7523-7535.	6.7	14
174	Effects of post-treatments on microstructure and hydrogen storage performance of the carbon nano-tubes prepared via a metal dusting process. Journal of Power Sources, 2008, 182, 317-322.	7.8	13
175	Influence of LiTFSI Addition on Conductivity, Diffusion Coefficient, Spin–Lattice Relaxation Times, and Chemical Shift of One-Dimensional NMR Spectroscopy in LiTFSI-Doped Dual-Functionalized Imidazolium-Based Ionic Liquids. Journal of Chemical & Engineering Data, 2015, 60, 471-483.	1.9	13
176	Roll-To-Roll Atomic Layer Deposition of Titania Nanocoating on Thermally Stabilizing Lithium Nickel Cobalt Manganese Oxide Cathodes for Lithium Ion Batteries. ACS Applied Energy Materials, 2020, 3, 10619-10631.	5.1	13
177	Hierarchical Interconnected Hybrid Solid Electrolyte Membrane for All-Solid-State Lithium-Metal Batteries Based on High-Voltage NCM811 Cathodes. ACS Applied Energy Materials, 2022, 5, 2580-2595.	5.1	13
178	Prior vacuuming for supercritical fluid synthesis of SnO2/graphene nanocomposites with superior electrochemical Li+ storage performance. Electrochimica Acta, 2018, 292, 951-959.	5.2	12
179	Effects of TiO2 and SDC addition on the properties of YSZ electrolyte. International Journal of Hydrogen Energy, 2019, 44, 29426-29431.	7.1	12
180	Determination of the Volume Changes Occurring for Conversion/Alloying-Type Li-Ion Anodes upon Lithiation/Delithiation. Journal of Physical Chemistry Letters, 2020, 11, 8238-8245.	4.6	12

#	Article	IF	CITATIONS
181	Physicochemical and electrochemical properties of the (fluorosulfonyl)(trifluoromethylsulfonyl)amide ionic liquid for Na secondary batteries. Journal of Power Sources, 2020, 470, 228406.	7.8	12
182	Atomic-scale investigation of Na3V2(PO4)3 formation process in chemical infiltration via in situ transmission electron microscope for solid-state sodium batteries. Nano Energy, 2021, 87, 106144.	16.0	12
183	Effects of alloying elements and binder on the electrochemical behavior of metal hydride electrodes in potassium hydroxide electrolyte. Journal of Solid State Electrochemistry, 2003, 7, 485-491.	2.5	11
184	The effect of surface structures and compositions on the quantum yields of highly effective Zn _{0.8} Cd _{0.2} S nanocrystals. Journal of Materials Chemistry C, 2015, 3, 5881-5884.	5.5	11
185	Facile electrochemical preparation of hierarchical porous structures to enhance manganese oxide charge-storage properties in ionic liquid electrolytes. Journal of Materials Chemistry A, 2016, 4, 4015-4018.	10.3	11
186	An Enhanced Electrode via Coupling with a Conducting Molecule to Extend Interfacial Reactions. Advanced Energy Materials, 2021, 11, 2101156.	19.5	11
187	Lithium Nafion–Modified Li _{6.05} Ga _{0.25} La ₃ Zr ₂ O _{11.8} F _{0.2} Trilayer Hybrid Solid Electrolyte for High-Voltage Cathodes in All-Solid-State Lithium-Metal Batteries. ACS Applied Materials & amp: Interfaces. 2022. 14. 15259-15274.	8.0	11
188	Hydrogen desorption behavior of vanadium borohydride synthesized by modified mechano-chemical process. International Journal of Hydrogen Energy, 2011, 36, 4993-4999.	7.1	10
189	Formation of metal coatings on magnesium using a galvanic replacement reaction in ionic liquid. RSC Advances, 2014, 4, 35298.	3.6	10
190	Copolymers Based on Indole-6-Carboxylic Acid and 3,4-Ethylenedioxythiophene as Platinum Catalyst Support for Methanol Oxidation. Catalysts, 2015, 5, 1657-1672.	3.5	10
191	Tuning oxidation level, electrical conductance and band gap structure on graphene sheets by a cyclic atomic layer reduction technique. Carbon, 2018, 137, 234-241.	10.3	10
192	Combinatorial Studies on Wet-Chemical Synthesized Ti-Doped α-Fe ₂ O ₃ : How Does Ti ⁴⁺ Improve Photoelectrochemical Activity?. ACS Applied Nano Materials, 2018, 1, 3145-3154.	5.0	10
193	Applications of Copolymers Consisting of 2,6-di(9H-carbazol-9-yl)pyridine and 3,6-di(2-thienyl)carbazole Units as Electrodes in Electrochromic Devices. Materials, 2019, 12, 1251.	2.9	10
194	Moderate-Concentration Fluorinated Electrolyte for High-Energy-Density Si//LiNi _{0.8} Co _{0.1} Mn _{0.1} O ₂ Batteries. ACS Sustainable Chemistry and Engineering, 2020, 8, 16252-16261.	6.7	10
195	High-voltage lithium-metal battery with three-dimensional mesoporous carbon anode host and ether/carbonate binary electrolyte. Carbon, 2021, 184, 752-763.	10.3	10
196	Electrodeposition of Al on Magnesium Alloy from Aluminum Chloride/1-ethyl-3-methylimidazolium Chloride Ionic Liquids. Electrochemistry, 2009, 77, 585-587.	1.4	9
197	High energy density layered-spinel hybrid cathodes for lithium ion rechargeable batteries. Materials Science and Engineering B: Solid-State Materials for Advanced Technology, 2016, 213, 148-156.	3.5	9
198	Designed Catalytic Protocol for Enhancing Hydrogen Evolution Reaction Performance of P, N-Co-Doped Graphene: The Correlation of Manipulating the Dopant Allocations and Heteroatomic Structure. Journal of Physical Chemistry C, 2020, 124, 25701-25711.	3.1	9

#	Article	IF	CITATIONS
199	A feasibility study of preparing carbon nanotubes by using a metal dusting process. Diamond and Related Materials, 2009, 18, 324-327.	3.9	8
200	Effects of scandium addition on electrical resistivity and formation of thermal hillocks in aluminum thin films. Thin Solid Films, 2011, 519, 3578-3581.	1.8	8
201	Effect of electrolyte temperature on the pseudo-capacitive behavior of manganese oxide in N-butyl-N-methylpyrrolidinium–dicyanamide ionic liquid. Journal of Power Sources, 2013, 233, 28-33.	7.8	8
202	Evolution of the sintering ability, microstructure, and cell performance of Ba _{0.8} Sr _{0.2} Ce _{0.8−} <i (<i>x</i> = 0.05, 0.1 <i>y</i> = 0, 0.1) proton-conducting electrolytes for solid oxide fuel cell. Journal of the Ceramic Society of Japan, 2015, 123, 193-198.</i 	sub>x& 1.1	amp;minus;y
203	High performance infrared heaters using carbon fiber filaments decorated with alumina layer by microwave-assisted method. Journal of the Taiwan Institute of Chemical Engineers, 2016, 59, 521-525.	5.3	8
204	Magnetic impurity effects on self-discharge capacity, cycle performance, and rate capability of LiFePO4/C composites. Journal of Solid State Electrochemistry, 2017, 21, 1767-1775.	2.5	8
205	Chemical stability and electrical and mechanical properties of BaZrxCe0.8-xY0.2O3 with CeO2 protection method. International Journal of Hydrogen Energy, 2017, 42, 22259-22265.	7.1	8
206	An assessment of pyrite thin-film cathode characteristics for thermal batteries by the doctor blade coating method. Journal of Materials Research and Technology, 2021, 13, 1139-1149.	5.8	8
207	Electrodeposition of Nanostructured Sn in 1-ethyl-3-methylimidazolium Dicyanamide Room Temperature Ionic Liquid. Electrochemistry, 2009, 77, 588-590.	1.4	7
208	Formation Mechanism of Self-Assembled Geâ^•Siâ^•Ge Composite Islands. Journal of the Electrochemical Society, 2011, 158, H1113.	2.9	7
209	Effect of Solvent on the Morphology of Nickel Localized Electrochemical Deposition. Journal of the Electrochemical Society, 2011, 158, D264.	2.9	7
210	Electrochemical deposition and pseudocapacitive behavior in urea-based quasi-ionic liquid electrolytes studied with X-ray absorption spectra. RSC Advances, 2012, 2, 9383.	3.6	7
211	Material characterization and electrochemical performance of Sr(Ce _{0.6} Zr _{0.4}) _{0.8} Y _{0.2proton conducting ceramics prepared by EDTA-citrate complexing and solid-state reaction methods. Journal of the Ceramic Society of Japan, 2015, 123, 187-192.}	>O <s 1.1</s 	sub>3&an
212	Primary human nasal epithelial cell response to titanium surface with a nanonetwork structure in nasal implant applications. Nanoscale Research Letters, 2015, 10, 167.	5.7	7
213	Mixed ionic liquid/organic carbonate electrolytes for LiNi0.8Co0.15Al0.05O2 electrodes at various temperatures. RSC Advances, 2015, 5, 106824-106831.	3.6	7
214	Analysis of an intermediate-temperature proton-conducting SOFC hybrid system. International Journal of Green Energy, 2016, 13, 1640-1647.	3.8	7
215	Ba1â^xSrxCe0.8â^yZryY0.2O3â^j^r protonic electrolytes synthesized by hetero-composition-exchange method for solid oxide fuel cells. International Journal of Hydrogen Energy, 2017, 42, 22222-22227.	7.1	7
216	Electrochemical energy storage of nanocrystalline vanadium oxide thin films prepared from various plating solutions for supercapacitors. Electrochimica Acta, 2018, 273, 257-263.	5.2	7

#	Article	IF	CITATIONS
217	Graphene induced crystallinity and hydrous state variations of ruthenium oxide electrodes for superior energy storage performance. Electrochimica Acta, 2020, 360, 136995.	5.2	7
218	High Power Na ₃ V ₂ (PO ₄) ₃ @C/AC Bi-material Cathodes for Hybrid Battery-Capacitor Energy Storage Devices. Journal of the Electrochemical Society, 2020, 167, 110546.	2.9	7
219	A Holey Graphene Additive for Boosting Performance of Electric Double-Layer Supercapacitors. Polymers, 2020, 12, 765.	4.5	7
220	Electrosynthesis of Electrochromic Polymer Membranes Based on 3,6-Di(2-thienyl)carbazole and Thiophene Derivatives. Membranes, 2021, 11, 125.	3.0	7
221	Improving high-temperature performance of lithium-rich cathode by roll-to-roll atomic layer deposition of titania nanocoating for lithium-ion batteries. Journal of Energy Storage, 2021, 44, 103348.	8.1	7
222	Oxygen reduction reactions from boron-doped graphene quantum dot catalyst electrodes in acidic and alkaline electrolytes. Journal of the Taiwan Institute of Chemical Engineers, 2022, 133, 104196.	5.3	7
223	Material characteristics and capacitive properties of aluminum anodic oxides formed in various electrolytes. Journal of Materials Research, 2004, 19, 3364-3373.	2.6	6
224	Costâ€Effective Hierarchical Catalysts for Promoting Hydrogen Release from Complex Hydrides. ChemSusChem, 2015, 8, 2713-2718.	6.8	6
225	Nano-fibrous SrCe0·8Y0·2O3-δ-Ni anode functional layer for proton-conducting solid oxide fuel cells. Journal of Power Sources, 2019, 436, 226863.	7.8	6
226	lonic Liquids with Various Constituent Ions To Optimize Non-Enzymatic Electrochemical Detection Properties of Graphene Electrodes. ACS Sustainable Chemistry and Engineering, 2019, 7, 16233-16240.	6.7	6
227	Germanium-assisted growth of titanium dioxide nanowires for enhanced photocatalytic and electron emission performance. Applied Surface Science, 2020, 530, 147204.	6.1	6
228	Electrodeposited Copolymers Based on 9,9â€2-(5-Bromo-1,3-phenylene)biscarbazole and Dithiophene Derivatives for High-Performance Electrochromic Devices. Polymers, 2021, 13, 1136.	4.5	6
229	New insights into interface charge-transfer mechanism of copper-iron layered double hydroxide cathodic electrocatalyst in alkaline electrolysis. Journal of Environmental Chemical Engineering, 2022, 10, 107287.	6.7	6
230	Different Types of Nanosized Carbon Materials Produced by a Metal Dusting Process. Journal of Physical Chemistry C, 2008, 112, 20143-20148.	3.1	5
231	Electrolyte Engineering: Optimizing Highâ€Rate Doubleâ€Layer Capacitances of Micropore―and Mesoporeâ€Rich Activated Carbon. ChemSusChem, 2017, 10, 3534-3539.	6.8	5
232	Amino-functionalization on graphene oxide sheets using an atomic layer amidation technique. Journal of Materials Chemistry C, 2020, 8, 700-705.	5.5	5
233	Electrosynthesis of electrochromic polymers based on bis-(4-(N-carbazolyl)phenyl)-phenylphosphine oxide and 3,4-propylenedioxythiophene derivatives and studies of their applications in high contrast dual type electrochromic devices. Journal of the Taiwan Institute of Chemical Engineers, 2022, 131, 104173.	5.3	5
234	Supercapacitive performance of porous graphene nanosheets in bis(trifluoromethylsulfony)imide and bis(fluorosulfonyl)imide ionic liquid electrolytes. Journal of Solid State Electrochemistry, 2018, 22, 2197-2203.	2.5	4

#	Article	IF	CITATIONS
235	Hydrous ruthenium oxide-tantalum pentoxide thin film electrodes prepared by thermal decomposition for electrochemical capacitors. Ceramics International, 2020, 46, 16636-16643.	4.8	4
236	Composites of platinum particles embedded into poly(6-cyanoindole)/poly(styrenesulfonic acid) for methanol oxidation. International Journal of Hydrogen Energy, 2021, 46, 16644-16654.	7.1	4
237	High-Power and Long-Life Na ₃ V ₂ O ₂ (PO ₄) ₂ F–Na ₃ V _{2 Bimaterial Electrodes for Hybrid Battery–Capacitor Energy Storage Devices. ACS Applied Energy Materials, 2022, 5, 4070-4084.}	2(P 5.1	O ₄ sub>4
238	Oxidation of Metallic Mn Thin Films Prepared in Butylmethylpyrrolidinium Bis(trifluoromethylsulfony)imide Ionic Liquid and the Pseudo-Capacitive Performance of the Anodized Oxides. ECS Transactions, 2008, 6, 165-174.	0.5	3
239	Enhanced Hydrogen Storage in MWCNTs Decorated by Electroless Nickel Nanoparticles Deposited in Supercritical CO ₂ Bath. Materials Science Forum, 2010, 638-642, 1148-1151.	0.3	3
240	Ionic Liquid-Modified Copper Phosphate Electrodes for the Detection of α-Amino Acids in a Weakly Alkaline Solution. Journal of the Electrochemical Society, 2016, 163, B768-B774.	2.9	3
241	Nanomechanical Properties and Fracture Behaviors of Ba1–xKxCe0.6Zr0.2Y0.2O3–δElectrolytes by Nanoindentation. Science of Advanced Materials, 2014, 6, 1691-1696.	0.7	3
242	High-Performance and Safe Hybrid Li-Ion Batteries Based on Li ₄ Ti ₅ O ₁₂ –TiO ₂ (A)–TiO ₂ (R)@C Anode and Na ₃ V ₂ O ₂ (PO ₄) ₂ F–Na ₃ V _{2 Cathode. ACS Sustainable Chemistry and Engineering, 2022, 10, 1390-1397.}	d 2(P	O ³ sub>4
243	Improvement on high-temperature electrochemical performance of lithium-ion pouch cells by spatial atomic layer deposition. Electrochimica Acta, 2022, 423, 140605.	5.2	3
244	Thermal stability of Ni(Ta) silicide films on ultra-thin silicon-on-insulator substrates. Journal of Alloys and Compounds, 2012, 536, S407-S411.	5.5	2
245	Electrodeposition of Nanomaterials. , 2017, , 835-895.		2
246	Electrochemical characteristics of 0.3Li2MnO3–0.7LiMn1.5Ni0.5O4 composite cathode in pyrrolidinium-based ionic liquid electrolytes. Journal of the Taiwan Institute of Chemical Engineers, 2019, 95, 195-201.	5.3	2
247	Hierarchical Carbon Composites for Highâ€Energy/Powerâ€Density and Highâ€Reliability Supercapacitors with Low Aging Rate. ChemSusChem, 2022, 15, .	6.8	2
248	Nitrogen-doped holey graphene additive for high-performance electric double-layer supercapacitors. Electrochimica Acta, 2022, 425, 140713.	5.2	2
249	Nano-Sized Carbon Materials Produced During the Metal Dusting Process of Stainless Steel and Their Hydrogen Storage Capability. ECS Transactions, 2007, 6, 45-54.	0.5	1
250	Preparation and Hydrogen Storage Performance of Pd Nanoparticles Decorated Carbon Nanotubes. ECS Transactions, 2009, 19, 33-40.	0.5	1
251	Creating electronic and ionic conductivity gradients for improving energy storage performance of ruthenium oxide electrodes. Journal of Alloys and Compounds, 2021, 862, 158013.	5.5	0
252	Improving the Electrochemical Performances of Supercapacitors through Modification of the Particle Size Distribution of the Carbon Electrode. IOP Conference Series: Earth and Environmental Science, 2021, 927, 012044.	0.3	0